# Photoionization Threshold of Eumelanosomes Determined Using UV Free Electron Laser−Photoelectron Emission Microscopy

**Alexander Samokhvalov,**[†] **Jacob Garguilo,**[‡] **W.-C. Yang,**[‡] **Glenn S. Edwards,**[§]
**Robert J. Nemanich,**[‡] **and John D. Simon\*,**[†,||]

*Chemistry Department, Duke University, Durham, North Carolina 27708, Physics Department,*
*North Carolina State University, Raleigh, North Carolina 27695, Free Electron Laser Laboratory,*
*Department of Physics, Duke University, Durham, North Carolina 27708, Biochemistry Department,*
*Duke University Medical Center, Durham, North Carolina 27708*

The application of UV-free electron laser photoelectron emission microscopy (UV-FEL PEEM) to measure the threshold photoelectron spectrum and photoionization potential for human eumelanosomes is described. The origin of potential artifacts and the limitations of the technique are discussed and their potential effects on the measured photoionization potential are quantified. The UV-FEL-PEEM images collected on human eumelanosomes isolated from black hair show that the organelle is photoionized by UV-B radiation. The photoionization threshold is determined to be 4.6 ± 0.2 eV. This result provides new insight into the origin of the differences between the photoionization and oxygen photoconsumption action spectra for eumelanins.

## Introduction

Photoelectron emission microscopy (PEEM) is an electron microscopy technique that images the electrons emitted from a surface illuminated by a beam of light. PEEM has been used to image various structures on metals and semiconductors.[1−4] Applications of PEEM to biological samples have also been extensively reviewed.[5−7] For most samples, PEEM requires an ultraviolet (UV) light source to achieve photoemission because most materials of interest have photothreshold energies in the 3−7 eV range.[8] In this respect, using a UV free electron laser (FEL) offers significant advantages in PEEM.[9]

In studying biological samples, one can apply PEEM in two different, yet complementary, ways. First, PEEM can be used solely for imaging, and the goal is to obtain high contrast between the features of interest in the image. PEEM imaging was applied to biological samples as early as 1972.[10] Since then, viruses and DNA,[11] eukaryotic cells,[6] cultured cancer cells,[12] and cytoskeletons[5] have been studied. Because PEEM is an ultrahigh vacuum technique, water must be excluded, and the samples must be fixed and dehydration or quick freezing is mandatory.[6] The majority of PEEM experiments were done on metal-coated or "stained" samples.[13] Coating with a highly photoemissive metal was required because biological samples are mostly insulators and therefore have a low photoelectric yield under the intensity of UV light commonly used. Such preparations exhibit excellent topographic contrast.[13] Because of this preparation procedure, caution must be exercised in correlating PEEM-observed structures with those of in vivo samples. PEEM imaging of fixed unstained biological samples

has also been reported,[14] but a common problem with unstained preparations is low electrical conductivity, which leads to image distortion due to charging.

Second, quantitative information on the electronic properties of the sample can be obtained. Photoemission quantum yields of several classes of biomolecules have been obtained using PEEM.[14,15] In these experiments, a suitable substrate is fully coated with the film of interest. The total photocurrent on a phosphor screen was measured with an attached electrometer when the photon energy of the exciting light was varied.[15] This allows determination of the absolute photoemission quantum yield. Photoemission quantum yields were reported for poly-(amino acids),[15] sugars, and some other biopolymers,[14] but no values for the threshold photoionization energies were reported. With a tunable light source, threshold photoionization energies can be determined. In the case where the biological sample contains a rich spatial structure, it is possible that the threshold ionization energy differs for the various constituents, and therefore wavelength-dependent PEEM images will provide both imaging information as well as variation in the chemical properties (ionization potential) within the imaged region.

Herein we use PEEM to study unstained human eumelanosomes isolated from black hair. Eumelanosomes do not require any fixation, dehydration, freezing, or staining to study by electron microscopy.[16] The dominant chemical constituent in eumelanosomes is the pigment eumelanin. The chemical structure of the pigment is not known; however early steps of eumelanogenesis are understood, and the pigment results from the oligomerization (and oxidation) of 5,6-dihydroxyindole and 5,6-dihydroxyindole-2-carboxylic acid.[17] In addition, human hair eumelanosomes contain protein (~14% be weight) and a variety of metal cations (~5 wt %).[18] Depending on the chemical composition and source of melanin, photoionization can occur either for wavelengths shorter than ~300 nm,[19] or under near-UV and even visible light.[20] In these previous works, synthetic melanin, not human melanosomes were studied. In addition, photoionized electrons were not directly observed, and instead,

\* To whom correspondence should be addressed: Department of Chemistry, Duke University, Box 90347, Duke University, Durham, NC 27708-0347. Phone: (919)-660-1630. Fax: (919)-660-1605. E-mail: jsimon@duke.edu.
  † Chemistry Department, Duke University.
  ‡ Physics Department, North Carolina State University.
  § Department of Physics, Duke University.
  || Duke University Medical Center.

Letters

*J. Phys. Chem. B, Vol. 108, No. 42, 2004* **16335**

their presence was inferred via adduct formation.[19] It remains to be determined whether melanosomes can be photoionized by near-UV or visible radiation, and more specifically, the value of the threshold photoionization potential.

Threshold photoionization potentials of solids are commonly determined by nonimaging wavelength-dependent photoemission techniques. Typically, the dependence of the photoelectron signal on excitation wavelength is measured for a macroscopically uniform sample. The Fowler equation is then used to calculate the threshold photoionization potential.[21] Examples of samples studied using this approach include semiconductors,[22] polymers,[23] organic solvents, and solutions.[24]

The technique of variable wavelength threshold PEEM was developed recently, which allows estimation of threshold photoionization potential of the given feature in a complex pattern on the surface.[9] However, absolute or relative photoemission quantum yield is not directly available from the data. Herein we describe a quantitative FEL-PEEM technique to obtain the threshold photoelectron spectra (or relative photoionization quantum yield) and the threshold photoionization potential of spatially nonuniform biological samples and report the resulting data for human eumelanosomes under varying conditions.

## Experimental Methods

**Sample Preparation.** Eumelanosomes were extracted and characterized as previously described.[18] Sections of silicon substrates (n-type, P-doped, resistivity $0.68-0.72\ \Omega$ cm, $9 \times 9$ mm$^2$) were cleaned by the standard RCA procedure prior to deposition of eumelanosomes.[25] This procedure results in a surface terminated with a $\sim$1 nm thick silicon oxide layer. Films were prepared by spreading the suspension of eumelanosomes in Nanopure water over the freshly RCA-cleaned Si wafer and allowing this to dry in air for less than 1 h. Under these conditions, films of eumelanosomes having irregular structure are obtained. Despite several attempts, we were unable to prepare continuous films.

A titanium surface was employed as a standard for the PEEM measurements. Sections of Si(001) wafers were cleaned by two cycles of UV−ozone exposure for 5 min followed by an HF (10%) dip for 1 min to remove hydrocarbon contaminants and the native oxide layers. The substrates were then mounted to the sample holder and introduced into the molecular beam epitaxy chamber (base pressure of $<1 \times 10^{-10}$ Torr), which is connected to the PEEM chamber. The substrates were submitted to a thermal treatment at 900 °C for 10 min to desorb any residual contaminants. A 10 nm thick layer of Ti was deposited at a rate of 0.1 nm/min by electron beam evaporation onto the cleaned surfaces at room temperature. The sample was then transferred under ultrahigh vacuum into the PEEM chamber.

**Photoelectron Emission Microscopy.** The photoemission electron microscope and the Duke UV-FEL light source have been described in detail previously.[9] We have utilized the spontaneous emission mode of the Duke UV-FEL in the spectral range 207−344 nm (6.0−3.6 eV), with an energy full width at half-maximum of $\sim$0.1 eV. The PEEM images were acquired with a DVC 1312M digital camera from DVC Company, Inc. (Austin, TX). The camera resolution is $1300 \times 1030$ pixel x 12 bits. The DVC View program was used to view/save images. We typically imaged assemblies of eumelanosomes at field of views in the PEEM of 150 $\mu$m, and single eumelanosomes at a field of view of 5 or 1.5 $\mu$m. The focusing of the FEL was optimized for each wavelength used; the FEL spot size on the sample was $\sim$30 $\times$ 100 $\mu$m.

**Image Analysis.** First, a PEEM image of the film at the given excitation wavelength was collected and saved as a graphic file. The total image size was typically $1292 \times 1030$ pixels. The file was opened in Irfan View image-processing software, and the desired image fragment was selected (e.g., an aggregate of eumelanosomes) and saved as a separate graphic file. The typical size of an image fragment was between 10 and 40 pixels in each dimension, corresponding to a few melanosomes, and significantly smaller than the spot size of FEL, and therefore, the irradiance at each pixel in the given image fragment was essentially constant.

A gray scale histogram (8 bits per pixel) of the image fragment was plotted by the Scion Image software, and the histogram was saved as an ASCII file. The X column of the histogram contains gray scale depths $i$ in units from 0 to 255 (8-bit scale), and the Y column contains the numbers of pixels $N(i)$ in the histogram, having the given gray scale depth $i$. This ASCII file with the gray scale histogram was opened with Microcal Origin software. The sum

$$S = \sum_i i*N(i) \tag{1}$$

was calculated. In this equation, $S$ equals the integrated brightness of the image fragment used, and this value is taken to be proportional to the photocurrent collected.

The ideal shape of the color histogram approaches a Gaussian distribution centered close to the middle of an abscissa ($i = 128$). Color histograms partially or completely located at $i = 0$ or $i = 255$ units were regarded as black or white color saturation, respectively. "Color saturation" is an artifact, and in this case the photoelectron current is not proportional to $S$. This was avoided by adjusting the software gain of the image acquisition program.

Three instrumental settings influence $S(\lambda)$: electron multiplication gain $G_h$ of the MCP electron multiplier ("hardware gain"), image-enhancing gain $G_s$ of the image-acquiring program ("software gain"), and incident laser power. If constant settings of $G_h$ and $G_s$ are used as the wavelength is scanned, $S(\lambda)$ changes considerably. This could lead to black or white color saturation. To avoid this, the software gain $G_s$ in the imaging program was adjusted and this was taken into account in determining $S(\lambda)$. In a few cases, the dynamic range available for $G_s$ was not sufficient to avoid color saturation, and $G_h$ was also adjusted. To calibrate the effect of $G_h$ on $S(\lambda)$, PEEM images were collected at fixed wavelength and software gain $G_s$, but with different hardware gains $G_h$. The ratio of $S(\lambda)$ provided the needed correction factor. $S(\lambda)$ also depends on the incident power at each wavelength. We measured the power of the FEL as function of photon energy at the input port of the PEEM chamber. $S(\lambda)$ was normalized to a constant fluence (photons/sec). We could not determine the light fluence on the sample within the PEEM microscope. Therefore, the wavelength-dependent data reveal relative, not absolute, photoionization quantum yield. The Fowler equation was used to calculate the threshold photoionization potential:[26]

$$S(\lambda)^{1/2} = C*(h\nu - \Phi) \tag{2}$$

In the above expression $C$ is constant and depends on the particular material studied, $\Phi$ is the threshold photoionization potential, and $h\nu$ is the photon energy. If a plot of $S(\lambda)^{1/2}$ as a function of $h\nu$ is linear, then the threshold photoionization potential $\Phi$ is obtained by determining the value of $\nu$ where $S(\lambda)^{1/2} \rightarrow 0$.
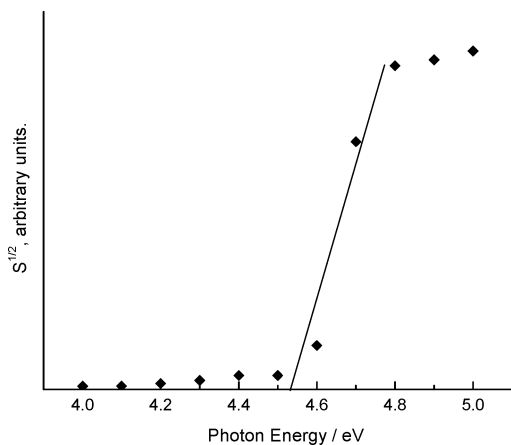
**Figure 1.** Square root of the brightness of the PEEM image, $S^{1/2}$, of a Ti film (10 nm thick) on Si(001) substrate plotted as a function of excitation wavelength. Extrapolation to $S(\lambda)^{1/2} \to 0$ gives a value for the threshold photoionization potential of $\sim 4.5 \pm 0.2$ eV.

## Results and Discussion

**PEEM of Ti on Si(001).** Figure 1 shows $S(\lambda)^{1/2}$ as a function of $h\nu$ for the Ti film on Si(001). The Ti film has a thickness of 10 nm and appeared uniform under PEEM imaging. This system served as a control experiment for the above-described analysis. Extrapolation to $S(\lambda)^{1/2} \to 0$ gives a value for the threshold photoionization potential of $\sim 4.5 \pm 0.2$ eV.

The reported work function of Ti is 4.33 eV,[27] which is in good agreement with this value. For a thin film, the underlying substrate can be photoionized and transmission of these electrons through the film would contribute to the PEEM signal. Si(001) is photoemissive for the short-wavelength region of the FEL output used. However, all photogenerated electrons would be scattered by a 10 nm thickness of Ti. UV light penetration is also short in metals, and a 10 nm film of Ti will efficiently absorb the incident UV light.[28] Thus, the electron signals originate from the Ti film and represent the electronic properties of Ti. We note that FEL light (spontaneous emission mode) is not monochromatic but has a bandwidth of 1% of the center wavelength. This results in a systematic error of <50 meV in the determined threshold value. This experiment serves to validate the above-described approach for determining the threshold photoionization potential from wavelength-dependent PEEM images.

**PEEM Images of Eumelanosomes.** Parts A and B of Figure 2 show an image of human hair and bovine eye retinal pigment epithelium eumelanosomes, respectively, on a Si substrate. Single melanosomes as well as aggregates are observed in these images. Hair eumelanosomes tend to aggregate more upon drying than the bovine retinal pigment epithelial melanosomes. Figure 3 shows a PEEM image of a single such bovine eye melanosome at a field of view of 1.5 $\mu$m, demonstrating that good quality images of single melanosomes can be obtained. The elongated shape with an aspect ratio of about 3 is well visualized. There are several small black spots, which are imaging artifacts due to damaged spots on the microchannel plate detector. The dark strip parallel to the long axis of the eumelanosome is attributed to a shadowing effect in PEEM.

**Threshold Photoionization Potentials.** The photoelectron signals from the single melanosome are weak for $\lambda \sim 250$ nm. To collect sufficient PEEM signals to carry out the determination of the threshold photoionization potential, an aggregate of eumelanosomes was imaged, and the $S(\lambda)$ for the total image was determined. These studies were restricted to the black-hair
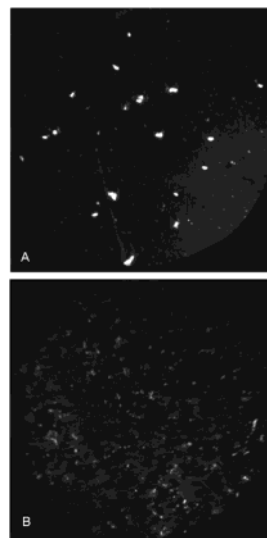


**Figure 2.** PEEM images of irregular films of melanosomes at $h\nu = 5.6$ eV: (a) human black hair melanosomes; (b) bovine retinal pigment epithelial melanosomes. Field of view is 150 $\mu$m.
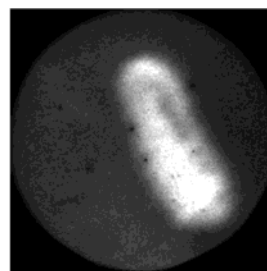


**Figure 3.** PEEM images of single bovine retinal pigment epithelial melanosome: field of view 1.5 $\mu$m, $h\nu = 240$ nm.
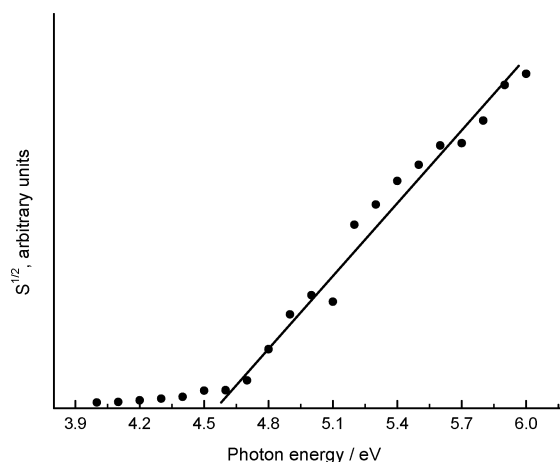


**Figure 4.** Square root of the brightness of the PEEM image, $S^{1/2}$, of black human hair melanosomes plotted as a function of excitation wavelength. Extrapolation to $S(\lambda)^{1/2} \to 0$ gives a value for the threshold photoionization potential of $\sim 4.6 \pm 0.2$ eV.

eumelanosomes. The wavelength-dependent threshold photoelectron spectrum using the full tuning range of FEL is shown in Figure 4. $S(\lambda)^{1/2}$ shows an essentially linear dependence on $h\nu$. Extrapolating $S(\lambda)^{1/2} \to 0$ gives a threshold photoionization potential to be $\sim 4.6 \pm 0.2$ eV. Various aggregates of eumelanosomes were examined. The results were independent of the particular aggregate studied.

The effect of the thickness of the eumelanosome deposit on the determined threshold photoelectron spectrum was also examined. Specifically, a submonomer film was compared to

Letters

*J. Phys. Chem. B, Vol. 108, No. 42, 2004* **16337**

one that consisted of ∼10 layers. Both showed a nearly linear dependence of $S(\lambda)^{1/2}$ versus $h\nu$. Extrapolating $S(\lambda)^{1/2} \rightarrow 0$ revealed the same threshold photoionization potential of as that reported above.

In UV-PEEM studies of photoelectron quantum yields of biomolecules, a sample thickness of several hundred nanometers is considered sufficient to completely block photoelectrons originating from the substrate.[15] Human black hair melanosomes are ellipsoidal in shape with long axis of ∼1 μm and an aspect ratio of ∼2.5.[18] So a single melanosome is thick enough to block photoelectrons from the underlying Si(001) substrate. Moreover, the exposed oxidized Si substrate would have a photothreshold of ∼5 eV.[29] The measured threshold photoionization potential therefore reflects the property of the melanosomes, independent of the film's regularity and thickness in the place of interest. As stated in the results section, within experimental error, the threshold photoelectron spectra were independent of the thickness of the film of melanosomes.

In addition to the artifacts discussed under the Ti/Si(001) model system, the following need to be considered in determining the accuracy of the threshold potential for the melanosomes by PEEM. First, in contrast to the Ti sample, the film of melanosomes is rough. The effect of sample roughness on the PEEM measurement is to decrease the value of the measured threshold photoionization potential compared with its true value. The origin of this effect is due to field enhancement, and one of the crucial parameters in determining the field enhancement is the aspect ratio of the topographic features.[8]

For the samples studied, there are two topographic aspect ratios: the intact melanosome and its fine structure. The black-hair eumelanosome is oval with an aspect ratio of ∼2.5.[17] In addition, there are nanoscale fine structures within the melanosome, whose aspect ratio does not exceed ∼2.[16] Therefore, the estimated largest aspect ratio for the samples of melanosomes is <3. This aspect ratio is similar to that recently studied for Cu features (dots and wavy lines) on Mo substrate.[9] These features cause a decrease in the measured work function by ∼200 meV from the established value for Cu films on Mo. Therefore, the roughness of this aspect ratio can cause an artifactual decrease of the measured threshold photoionization potential by ∼200 meV.

Second, the strong electric field at the surface of the sample leads to a lowering of the electron emission barrier, an effect that is commonly referred to as the Schottky effect. The barrier $(e\Delta\phi)$ is lowered by[30]

$$e\Delta\phi = e\sqrt{\frac{eE}{4\pi\epsilon_o}} \tag{3}$$

In the above expression $E$ is the applied accelerating field in the PEEM and $\epsilon_o$ is the permittivity of free space. In the FEL-PEEM experiments, $E = 100$ kV/cm and $e\Delta\phi = \sim120$ meV. Thus, taken together, the roughness artifact and the Schottky effect could reduce the value of threshold photoionization potential by ∼300 meV.

**Implications for Eumelanosomes.** In the FEL-PEEM experiment, the melanosomes are photoionized under vacuum, and thus the photoionization potential is referenced to the vacuum level. The potential of an electron at rest in a vacuum corresponds to −4.44 V versus NHE[31] and so the oxidation potential of eumelanosomes vs NHE is ∼−0.2 V. Though one must be careful in comparing potentials measured for intact melanosomes with those of synthetic melanin, it is interesting to note that the electrochemical $E_{1/2}$ potential for the thin films

of 5,6-dihydroxyindole−melanin is 125 mV versus Ag/AgCl, which was attributed to the quinine−imine couple.[32] Cyclic voltammetric measurements of synthetic dopamine melanin at pH 5.6 reveals two main peaks in oxidation at +460 and +525 mV versus SCE.[33] Both measurements on synthetic systems are in reasonable agreement with that determined in the present study for the intact eumelanosome.

The action spectrum for the photoionization of bovine eye eumelanosomes was obtained by electron spin resonance spin-trapping experiments. The apparent threshold for photoionization was found to be about 4.1 eV (∼300 nm).[19] The measurement herein on human eumelanosomes is 4.6 eV (270 nm), which is in reasonable agreement with the previous observations. It is interesting to note the action spectrum for photoionization reported by Kalayanaraman et al. is in good agreement with the action spectrum of oxygen photoconsumption for wavelengths $\lambda < 250$ nm.[19] However, unlike the photoionization action spectrum, the action spectrum of oxygen photoconsumption exhibits a tail at $\lambda > 250$ nm, i.e., in the UV-B and -A regions, with an offset of about 2.5 eV (∼500 nm).

The agreement between the two action spectra for $\lambda < 250$ nm strongly supports a conclusion that the first step of oxygen activation is photoionization of the melanosome, followed then by scavenging by molecular oxygen to form the superoxide radical anion. But the differences between the photoionization and oxygen photoconsumption action spectra for $\lambda > 250$ nm seem to imply a different mechanism is involved in oxygen activation in this wavelength region.

However, the differences between these action spectra can be attributed to the properties of intact melanosomes and dissolved oligomers, and not a change in reaction mechanisms with different excitation wavelengths. Specifically, we previously demonstrated the action spectrum for the photoconsumption of oxygen agrees quantitatively with the absorption spectrum of the small oligomeric subunits (molecular weight less than 1000 amu) that comprise the eumelanin pigment in both hair and Sepia.[34,35] Furthermore, aggregation of these oligomeric species mitigates the generation of reactive oxygen species.[36] We therefore attribute the differences between the photoionization and oxygen photoconsumption action spectra to the reactivity of oligomeric species that were solubilized in the sample preparation as compared to experiments on intact melanosomes.

In conclusion, the photoionization threshold of human eumelanosomes isolated from black hair determined to be 4.6 ± 0.2 eV using UV-free electron laser photoelectron emission microscopy. This result is in reasonable agreement with electrochemically measured oxidation potentials of melanin samples, as well as with the threshold for the action spectrum of photoelectron generation of melanosomes in solution. These studies establish that FEL-PEEM can be a powerful technique for characterizing the electrochemical properties of pigments.

**References and Notes**

(1) Mundshau, M.; Swiech, W.; Bauer, E. *J. Appl. Phys.* **1988**, *65*, 581.

(2) Rotermund, H.; Nettesheim, S.; Von Oertzen, A.; Ertl, G. *Surf. Sci.* **1992**, *275*, L645.

(3) Yang, W.-C.; Rodriguez, B. J.; Park, M.; Nemanich, R. J.; Ambacher, O.; Cimalla, V. *J. Appl. Phys.* **2003**, *94*, 5720.

(4) Yang, W.-C.; Zeman, M.; Ade, H.; Nemanich, R. J. *Phys. Rev. Lett.* **2003**, *90*, Art. No. 136102

(5) Birrell, G. B.; Hedberg, K. K.; Habliston, D. L.; Griffith, O. H. *Ultramicroscopy* **1991**, *36*, 235.

(6) Griffith, O. H.; Rempfer, G. F. *Annu. Rev. Biphys. Biophys. Chem* **1985**, *14*, 113.

(7) Griffith, O. H.; Habliston, P. A.; Birrell, G. B. *Appl. Surf. Sci.* **1986**, *26*, 265.

(8) Yang, W.-C. Ph.D. thesis, North Carolina State University 2001, p 17.

(9) Ade, H.; Yang, W.; English, S. L.; Hartman, J.; Davis, R. F.; Litvinenko, V. N.; Pinaev, I. V.; Wu, Y.; Madey, J. M. J.; Nemanich, R. J. *Surf. Rev. Lett.* **1998**, *5*, 1257.

(10) Griffith, O. H.; Lesch, G. H.; Rempfer, G. F.; Birrell, G. B.; Burke, C. A.; Schlosser, D. W.; Mallon, M. H.; Lee, G. B.; Stafford, R. G.; Jost, P. C.; Marriott, T. B. *Proc. Natl. Acad. Sci. U.S.A.* **1972**, *69*, 561.

(11) Birrell, G. B.; Habliston, D. L.; Griffith, O. H. *Biophys. J.* **1994**, *67*, 2041.

(12) Habliston, D. L.; Hedberg, K. K.; Birrell, G. B.; Rempfer, G. F.; Griffith, O. H. *Biophys. J.* **1995**, *69*, 1615.

(13) Nadakavukaren, K. K.; Rempfer, G. F.; Griffith, O. H. *J. Micros-copy* **1981**, *122*, 301.

(14) Dam, R. J.; Nadakavukaren, K. K.; Griffith, O. H. *J. Microscopy* **1977**, *111*, 211.

(15) Griffith, O. H.; Holmbo, D. L.; Habliston, D. L.; Nadakavukaren, K. K. *Ultramicroscopy* **1981**, *6*, 149.

(16) Liu, Y.; Simon, J. D. *Pigm. Cell Res.* **2003**, *16*, 606.

(17) Ito, S. *Biochim. Biophys.* **1986**, *883*, 155.

(18) Liu, Y.; Kempf, V. R.; Nofsinger, J. B.; Weinert, E. E.; Rudnicki, M.; Wakamatsu, K.; Ito, S.; Simon, J. D. *Pigm. Cell Res.* **2003**, *16*, 355.

(19) Kalayanaraman, B.; Felix, C. C.; Sealy, R. C. *J. Am. Chem. Soc.* **1984**, *106*, 7327.

(20) Chedekel, M. R.; Land, E. J.; Sinclair, R. S.; Tait, D.; Truscott, T. G. *J. Am. Chem. Soc.* **1980**, *102*, 6587.

(21) Fowler, R. H. *Phys. Rev.* **1931**, *38*, 45.

(22) Benemanskaya, G. V.; Daineka, D. V.; Frank-Kamanetskaya, G. E. *J. Phys.: Condens. Matter.* **1999**, *11*, 6679.

(23) Mochida, K.; Shimoda, M.; Kurosu, H.; Kojima, A. *Polyhedron* **1994**, *13*, 3039.

(24) Watanabe, I. *Anal. Sci.* **1994**, *10*, 229.

(25) Senturia, S. D. *Microsystem Design*; Kluwer Academic Publish-ers: Boston, 2001.

(26) Rapp, M.; Luebken, F.-J. *Earth Planet Space* **1999**, *51*, 799.

(27) van der Heide, P. A. W. *Surf. Sci.* **1995**, *341*, 150.

(28) Pankove, J. I. In: *Photoemission in Solid*; Cardona, M., Ley, L., Eds.; Dover Publications: New York, 1978.

(29) Fulton, C. C.; Lucovsky, G.; Nemanich R. J. *J. Vac. Sci, Technol. B* **2002**, *20*, 1726.

(30) Murr, L. E. *Electron and Ion Microscopy and Microanalysis*; Marcel Dekker Inc.: New York, 1991.

(31) Graetzel, M. *Nature* **2001**, *414*, 338.

(32) Gidanian, S.; Farmer, P. J. *J. Inorg. Biochem.* **2002**, *89*, 54.

(33) Serpentini, C.-L.; Gauchet, C.; de Montauzon, D.; Comtat, M.; Ginestarand, J.; Paillous, N. *Electrochim Acta* **2000**, *45*, 1663.

(34) Nofsinger, J. B.; Forest, S. E.; Simon, J. D. *J. Phys. Chem. B* **1999**, *103*, 11428.

(35) Nofsinger, J. B.; Weinert, E. E.; Simon, J. D. *Biospectroscopy* **2002**, *67*, 302.

(36) Nofsinger, J. B.; Liu, Y.; Simon, J. D. *Free Rad. Biol. Med.* **2002**, *32*, 720.